Control of the Gas-Phase Composition (of Atmospheric Pressure Air Plasmas) Using Pulsed Dielectric Barrier Discharges

Ruggero Barni , Prince Alex , Claudia Riccardi *

Posted Date: 17 October 2023

doi: 10.20944/preprints202310.1005.v1

Keywords: Dielectric Barrier Discharge; Atmospheric Pressure Plasmas; Chemical Kinetics; Plasma Modeling

Article

Control of the Gas-Phase Composition (of Atmospheric Pressure Air Plasmas) Using Pulsed Dielectric Barrier Discharges

Ruggero Barni [1], Prince Alex [1,2] and Claudia Riccardi [1,*]

[1] Dipartimento di Fisica, Università degli Studi di Milano-Bicocca, Piazza della Scienza 3, 20126 Milano, Italy; ruggero.barni@mib.infn.it (R.B.); princealexanderm@gmail.com (P.A.)
[2] Department of Physics, St. Joseph's College Devagiri, Calicut-673008, India
* Correspondence: claudia.riccardi@unimib.it.

Featured Application: Control or at least prediction of the gas-phase composition in atmospheric pressure cold plasmas is key to evaluate the potential of plasma treatments, which could be considered in several applications, from health and environmental processes targeting hazard agents to production of advanced materials through suitable surface functionalization.

Abstract: We presents results obtained from the numerical simulation of the gas-phase chemical kinetics in atmospheric pressure air non-equilibrium plasmas. In particular we have addressed the effect of pulsed operation mode of a planar dielectric barrier discharge. As it was conjectured, the large difference in the time scales involved in the fast dissociation of molecules in plasmas and their subsequent reactions to produce stable chemical species, makes the presence of a continuously repeated plasma production stage unnecessary and a waste of electrical power and efficiency. Results on NOx remediation, ozone production, water vapor and ammonia dissociation are discussed. A few comparisons with experimental findings in a dielectric barrier discharge reactor already used for applications is briefly addressed too. Our results clearly indicate a pattern for the optimization of the discharge using a carefully designed repetition rate and duty-cycle.

Keywords: dielectric barrier discharge; atmospheric pressure plasmas; chemical kinetics; plasma modeling

1. Introduction

Dielectric Barrier Discharges (DBD) have been widely employed in devices to obtain non equilibrium plasmas at or near atmospheric pressure, with a limited power consumption [1–5]. Their main feature is the auto-regulation of the electric current intensity and of the gas temperature, which is obtained by avoiding any direct pattern through the gas gap joining the electrodes, usually interposing some dielectric materials between them. The discharge electric current is regulated by its delivery of charges accumulating on the insulating surfaces, counterbalancing the externally applied electric fields and quenching the electrical breakdown [1]. At or near atmospheric pressure the discharge develops into narrow filaments where an ionizing wave is propagating along their axis, usually having small transverse sizes. The duration of the discharge process is usually very short, whereas the charge density could quite high [1]. The steady state operations required by applications can be achieved by a repetition, on average periodical, of such discharge events filling, in the best case uniformly, the gas gap. To remove the charge accumulated in the discharge region and its surrounding surfaces, the discharge is normally sustained by applying an oscillating voltage to one of the electrodes at kHz frequencies, although different waveforms of HV signal and even unipolar pulses can be employed. In the simplest situation, the changing sign voltage dissipates away the charge deposited on the dielectric surfaces and a new filament with the current flowing in the other way could originate from the same location on the insulating material. What we would like to point

 doi:10.20944/preprints202310.1005.v1

out is that each of such discharges is very brief with intervals of dead times between an event and another. On the other side, they appear as separated also regarding the space location, since, at least in small gaps, they develops in very slim channels (with typical radii R about a hundred micrometres [2]) whereas their separation is generally much larger, in the order of the gap size and so a few millimetres [1,2].

The relevant observation, concerning our topic, is that in a such environment the local gas-phase composition gets controlled both by the happening of one of the discharge paths (usually a very fast phenomenon) but also by the duration of the quiet time intervals between two consecutive such events. At later times, diffusion both perpendicular and parallel to the discharge filament paths leads to mixing and equlization of the gas-phase, followed by the macroscopic diffusion, or advection if present, from the whole discharge region. The main topic we would like to investigate here is whether the interplay between the two phases could be altered and somewhat directed by delivering the discharges in time bunches, using suitable duty cycles, a task that could be provided by advanced pulsed HV generators [6,7].

To this purpose we have reformulated our previous model, which simulates the chemical kinetics of atmospheric pressure discharges produced by DBD devices [8,9], in order to embody the effect of a pulsed operation mode on the gas phase composition. We have then studied a few suitable cases, where pulsed operation could have an impact.

The paper was structured as follows. At first we present the numerical simulation of the chemical kinetics in the gas-phase of a single air microdischarge. Then we discuss the results of the numerical study of pulsed operation in a DBD reactor, taking into account the effects of multiple discharges and of duty cycles on the development of the gas-phase chemistry. We then present some case studies. In particular we discuss the dynamics of ozone, one of the main discharge output and how this is modified by the pulsed operation mode. In the context of Volatile Organic Compound (VOC) remediation, we discuss the prospect of abatement of nitrogen oxides by pulsed DBD. Finally, using an extended model suitable for simulations of plasmas in humid air, we present some observations concerning the chemical kinetics of water vapour and ammonia in a pulsed DBD reactor.

In the end we discuss the findings of an experimental campaign, aimed to VOC remediation and air purification [10,11]. Targeted simulations, mirroring at best the experimental conditions, have been performed to compare actual results with the numerical predictions.

2. Materials and Methods

Our aim was to develop a framework suitable to investigate the gas-phase composition of an atmospheric pressure discharge, as it develops in a DBD reactor. There multiple breakdown events happen and repeat in different, but partially superimposing, space locations and times. The main point is whether this superposition could be exploited to control the evolution of the discharge gas-phase composition and thus tailoring the production or destruction rate of specific targeted compounds. The first step was to formulate a simplified model that allows to simulate the microdischarge formation [8]. Then we addressed the task to take into account the effects arising from the reiterated applications of several discharge events according to some definite spatial and temporal pattern.

As already mentioned, the electric discharge in DBD is made up of narrow current filaments each having lifetimes of a few nanoseconds. They can be modeled as isolated events in time and space. Several models [12–15] and many experimental details [16–20] have been collected to get a picture of the formation, development and propagation of these events, which show a remarkable common character even in different kind of DBDs [1]. The development of the discharge filaments is guided by the electron avalanche multiplication that happens in the strong field ahead of the ionizing wave (which could reach values about 5–15 × 10^6 V/m) and which travels typically very fast (with velocities in the 10^5–10^6 m/s range). The discharge filament body then consists of a thin channel of weakly ionized gas, almost quasi-neutral (with densities $n_+ \sim n_-$ of the order of 10^{13}–10^{15} cm^{-3}). When the spreading ionization area reaches the insulator material that prevents the direct contact with the

Preprints (www.preprints.org) | NOT PEER-REVIEWED | Posted: 17 October 2023 doi:10.20944/preprints202310.1005.v1

cathode pole, the conductive ionized gas supports a small electrical current, which is quickly decaying because of the nearby space charge located at the dielectric surface [1].

Having this in mind, we could focus on what happens at a fixed position along the discharge filament path. The picture is that the electric field will increase very quickly from its local unperturbed value as the ionizing wave gets approaching and then it decays almost as fast to the much smaller value it assumes in the filament channel. In fact, it should be remembered that at high pressures electrons moves along the electric field at the drift velocity and almost instantaneously (ν_m^{-1} ~ 0.3 ps, ν_E^{-1} ~ 50 ps [21]) reach a mean energy determined by the amplitude of the field there. This behavior will control both the filament propagation and the ionization strength. On the other hand ion inertia keeps them practically still and substantially cold, that is almost at the set temperature. The effect then will be that of an ionizing wave quickly propagating between the two dielectric surfaces, with the local charge density increasing as the wave passes by. This affects not only the formation of the discharge filament, but also the chemical composition of its gas-phase. Indeed, from the chemical kinetics point of view, the process can be seen as consisting of an almost instantaneous phase during which energetic electrons produce new electrons and ions, but also atoms and more generally radicals, out of the impact dissociation processes on the initial gas-phase molecules. This event is followed by a phase in which electrons cool down very quickly and reach lower temperatures, effectively ending the efficient fragmentation conditions. It should be pointed out that existing models could be used to predict the distribution and the intensity of the electric field pulses during their movement in the gas gap, depending from the electrode geometry and initial gas-phase composition [11,12]. The general picture, however, shows that the dependence from the position along the filament path is not so large, apart from the region near the dielectric surface. So, in order to keep complexity small, we have chosen to neglect such differences and we have formulated the model assuming uniformity along the filament path. To simplify geometry at most, the filament body was idealized as that of a thin cylinder, with a circular cross-section. The numerical value of the radius has to be considered as one of the free, tunable parameters of the simulation, even if here we have considered a value of 100 μm as the reference, as discussed above [21]. The cylinder height, that corresponds to the discharge gap, was set to 0.8 mm, somewhat typical and equal to a few previously performed laboratory experiments. [22]. A second approximation was introduced to treat the ionizing wave. In the model it was idealized as a a pulse of the electric field strength uniform in the head of the developing filament. The pulse is therefore characterized only by an electric field amplitude E_{max} and by the duration τ_s of it (about 2 ns, based on the model in ref. [11]). Although a bit rough, such a simplification embodies all the relevant phenomena for our aims. This saves a lot of time and reduces complexity, since we have not to recalculate the ionization and dissociation rates during the ionizing wave passage. A tricky point needs a little more clarification. At the start of the simulation, as the ionizing wave arrives, the electron density starts to increase very strongly, almost exponentially. Because of this behavior, the total amount of ions and radicals produced during the wave passage is set mainly by the actual value reached by the electron density at the end of the pulse [9]. In practice it happens to be largely independent from the time length of the ionizing wave and from the initial electron density. So the value of τ_s was fixed to 2 ns, in these simulations. The truly variable parameters was then the electron density reached after the passage of the ionizing wave. As a reference we considered a density of 1.2×10^{14} cm^{-3}, based on the typical charge transported by microdischarges, of about 0.7 nC [10,23].

Thanks to the approximations introduced, the model can be classified, from a chemical engineering point of view, as a well-mixed reactor with cylindrical geometry [24]. A further approximation is applied to treat the spatial profiles of the concentrations of the different chemical species. Because of the assumed uniformity along the filament axis, diffusion along this direction is neglected and concentrations are independent from the axial coordinate. The transverse profile of the concentration is described in terms of the normal modes dictated by the geometry, here, as already stated, a cylindrical one [25]. The gas-phase composition in the reactor is determined by the concentrations of the different N species considered by the model, which now only depend from time. Their time evolution is controlled by the balance between the chemical reactions involving the

Preprints (www.preprints.org) | NOT PEER-REVIEWED | Posted: 17 October 2023 doi:10.20944/preprints202310.1005.v1

reactive species and the transport processes. It could be calculated by integrating each balance equation for the density n_k of the k^{th} species:

$$\frac{dn_k}{dt} = \sum_{i<j=1}^{N} K(i+j \rightarrow k)\, n_i n_j - \sum_{i,j=1}^{N} K(k+i \rightarrow j)\, n_k n_i + \frac{D_k}{\Lambda_k^2} n_k \qquad (1)$$

Here K are the reaction rates for the gas phase reactions including those involving electrons and ions, whereas D and Λ are the diffusion coefficient and effective length [25]. In particular, the coefficient Λ depends only on geometrical factors and on the sticking coefficient S of each chemical species [25]. Adsorption on the dielectric barrier could easily be included but, because of the much smaller extension of the filament radius respect to the discharge gap, it turns out to be negligible, apart from ions. Since all the coefficient are constant, the above mentioned equations form a system of coupled differential equations which has been integrated by using an adaptive Runge-Kutta routine [8].

The choice of ions and molecules to be included in the model was based on existing experimental data based on emission spectroscopy or mass spectroscopy. For atmospheric air, here we considered only oxygen and nitrogen species, in a 20:80 mixture. A set of 10 neutral, including different nitrogen oxides, 10 metastables and 9 charged species was included in the simulations presented here. Rate constants for neutral gas-phase, charge exchange and ion recombination reactions have been taken from literature referenced in [8,9]. A strict cold plasma approximation is used. So reaction rates for ion as well as neutral species are evaluated at the set temperature, that is 300 K, even if this could be changed if needed for comparison with experiments. In atmospheric pressure air plasmas neutral rates depend also from the vibrational states of molecules, in particular those of nitrogen molecules [26,27]. This aspect could be taken partially into account considering a mean energy associated with vibrational states (usually referred to as the vibrational temperature) and updating the reaction rates accordingly [9,28]. Such a rough approximation avoid an overwhelming multiplication of the species numbers and of often largely unknown reaction rates, by considering separately the individual vibrational states. From the previous discussion, it is clear the central role played by electron-impact reactions, whose rates used in this study have been already discussed in our previous works too [8,9]. For a reason of simplicity, such rate constants have been evaluated assuming a Maxwellian energy distribution function for electrons, described then by only one parameter, their temperature T_e. This could be better thought of as a determination of the mean electron energy, which in turn is linked to the local electric field value, through the Boltzmann equation [21]. This value should be used in order to make a direct comparison between this simulation and other ones or with the experimental measurements. So, instead of a specific value of the electric field strength E_{max} in the ionizing wave pulse, we have considered as reference an electron temperature value of 4 eV [8]. Together with the electron density, those are the two main parameters used to perform simulations and discussed below. By the way, a total of 410 reactions and 43 diffusion processes have been taken into account in the simulations.

3. Results

In order to grasp the relevant time scales in the build-up of the plasma gas-phase, we present the results of a simulation that models the evolution of a single discharge happening once. Both neutral and ion species densities are shown as a function of time respectively in Figure 1a for stable species, Figure 1b for charged species and Figure 1c for metastable neutral states. Throughout the whole paper we will use double logarithm scales. This allows to appreciate the evolution also of minority ions and molecules and their build-up during times. It also permits to appreciate the effects of the fast ionizing wave together with the slower features connected with chemical reactions, repetitions and diffusion processes.

Preprints (www.preprints.org) | NOT PEER-REVIEWED | Posted: 17 October 2023 doi:10.20944/preprints202310.1005.v1

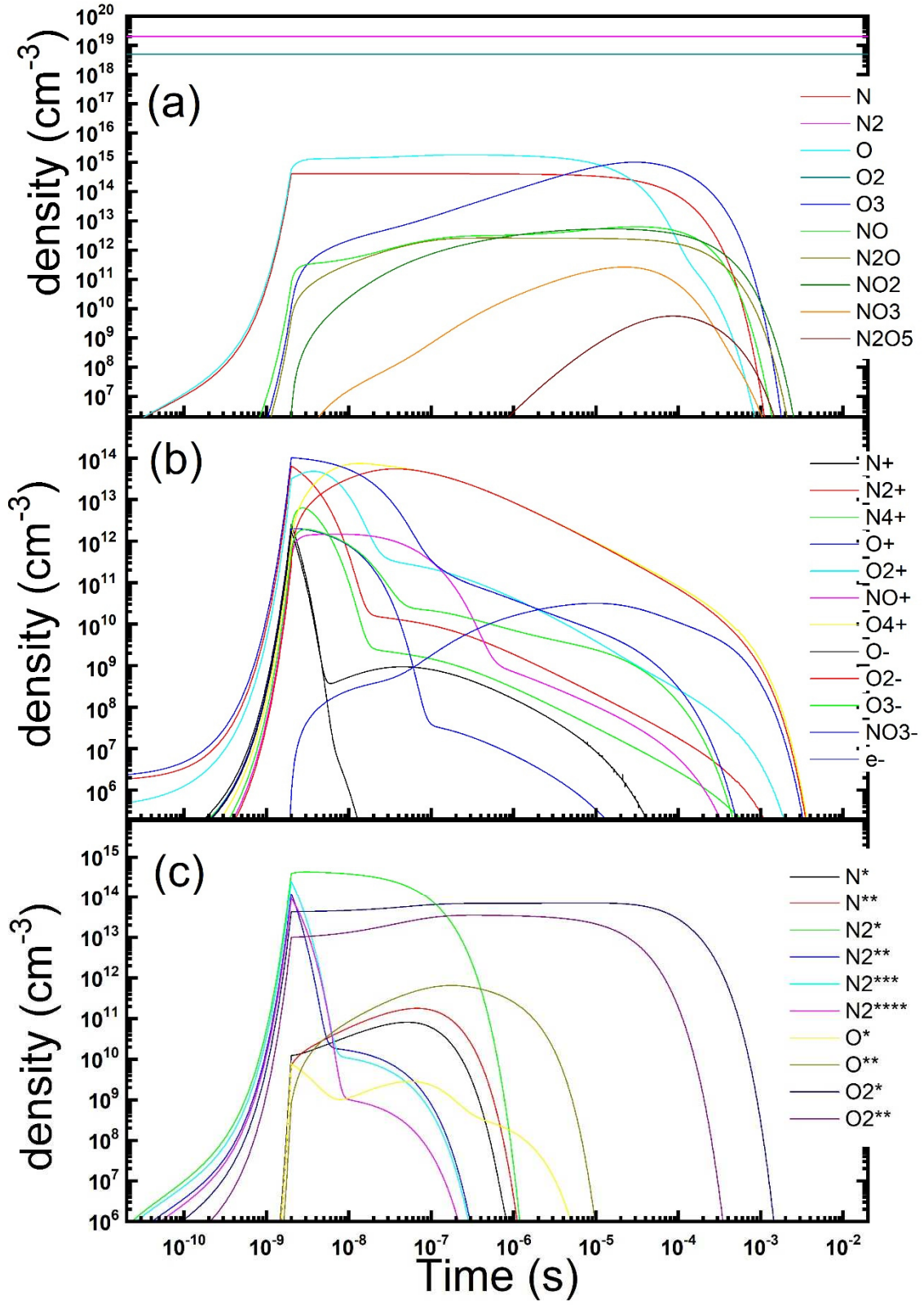

Figure 1. Temporal evolution of the gas phase composition during and after a microdischarge in dry air: neutrals (**a**), charged (**b**) and metastables (**c**) species concentration is reported (parameters: $T_e = 4$ eV, $n_e = 1.2 \times 10^{14}$ cm^{-3}, $\tau_s = 2$ ns, $R_{str} = 100$ μm, $D_{gap} = 0.8$ mm).

Preprints (www.preprints.org) | NOT PEER-REVIEWED | Posted: 17 October 2023 doi:10.20944/preprints202310.1005.v1

As it could be expected, during the time length τ_s (2 ns) needed for the ionizing pulse sweep, O and N atoms are produced, in the dissociation from parent molecules by electron collisions (oxygen atoms density exceeds nitrogen one as predicted at the chosen value of the electron temperature). Subsequently the development of the gas-phase starts. It turns out that ozone is continuously produced until its density becomes of the same order of that of the atoms. Afterwards atomic oxygen density decays, as atoms are substituted by ozone as the main product in the gas phase. Ozone exceeds oxygen atoms after sometimes at 11 μs. The peak density reached by ozone was about 1.1×10^{15} cm^{-3} after about 32 μs. Subsequently the diffusion processes kick in. They are able to sweep away the whole modified gas phase in some milliseconds. Nitrogen oxides accumulates too, albeit at a somewhat slower rate because of the lesser reactivity of nitrogen, staying always minority in the gas-phase. The composition of the charged species is much more complex. First of all, the temporal dynamics of charged species appears to be faster than that of neutrals. This is mostly due to the higher rates of ion-ion recombination, charge exchange reactions and of electron attachment. As expected, all the charged species increase almost exponentially during the streamer development time (2 ns). Afterwards the total charge density begins to decrease because of recombination. Another two processes happen to modify the charged gas-phase. In presence of oxygen, after the pulse ends, when the electron temperature decreases below than about 2 eV, electrons get quickly removed due to attachment processes. Under the reported setting the O_2^- molecule turns out the main negative ion and the overcoming happens after just 14 ns. On the other hand, positive charged species composition is mainly determined by charge exchange reactions on the still majority N_2 and O_2 molecules. They quickly remove atomic ions and leave O_4^+ as the majority ion. In our condition, this substitution is even readier than that of the electrons. Subsequently ions density, both positive and negative charged species, displays the same trend: a decrease in time (formally described by a power-law that appears as a straight line in our logarithm scale pictures) controlled by the ion-ion recombination process, followed by a decay due to diffusion towards the dielectric surfaces (formally described by a negative exponential curve), when density decreases at such low values that recombination becomes negligible respect to transport. At the minority level, we observe also a brief time window where formation of NO^+ ion is observed, together with its subsequent removal. Excited molecules are produced during the passage of the ionization wave, just as ions and dissociated atoms. Most of them are quickly quenched by reactions in the gas-phase or radiative decay after the end of the ionization phase. Metastable, weakly interacting states remain in the discharge gas-phase. Their lifetime is determined by the slower quenching reactions. The most lasting are metastable molecular oxygen states which accumulate in the gas phase discharge. The last one is removed by diffusion together all the other discharge products. We could observe also that metastable atomic states start accumulating only after the production of a suitable amount of the parent atoms and remain minority in the chosen conditions.

When the discharge happens more times, that is we introduce a repetition at a defined frequency (above the kHz range) the interplay between the dissociation and formation of oxygen atoms and the reactions in gas phase leading to the ozone production is exposed. The density of the same neutral and charged species considered before is displayed in the same logarithm scale as a function of time in Figure 2, considering a repetition period of 25 μs. To ease comparison, only the densities calculated at the end of each discharge are reported on the graph at later times. These conditions correspond to a symmetric DBD fed by a supply with a 20 kHz sinusoidal HV signal. The first observation is that after a very small number of repetitions, in the order of ten, the gas phase reaches a steady composition at the end of each discharge. Since the repetition rate chosen is longer than the ozone overcoming times, this is the species that dominates the gas-phase. More specifically, an equilibrium is reached between the ozone produced in the post discharge phases and that removed by diffusion or destroyed in the discharges. Under such conditions ozone reaches a steady state concentration of about 4.7×10^{15} cm^{-3} (about 180 ppm) whereas atomic nitrogen and oxygen densities are ten times smaller and nitrogen oxides more than one hundred less. The same picture is reported also for charged and excited species. Although the overall behaviour is similar to that already reported, we could notice that minority negative ions could accumulate now, because of the repetitions. As for the metastable states, accumulation happens only, as expected, for the species whose quenching time is longer enough, respect to the repetition period. A deeper analysis shows that the key timing is

 doi:10.20944/preprints202310.1005.v1

whether the repetition frequency allows the multiple discharges to happen after the overcoming of atomic oxygen by ozone but before the diffusion has kicked in. By tuning the time interval between multiple discharges it is possible to define an optimal periodicity under which the ozone flow outside the discharge region is maximal. This condition roughly correspond to the one when the maximal concentration is reached at the end of the discharge. However this condition has not to be considered as the best production of ozone achievable, since one could observe that the multiple repetition of discharges has also the effect to destroy a fraction of the ozone formed in the time after the previous discharge. This is way we are up to consider whether a duty cycle operation mode could affect and possibly increase for instance the ozone production. On the other hand, continuous operation implies steady energy injection and thus consumption, even where sufficient active species are already present and not really needed to increase stable species, notably ozone, build-up.

Preprints (www.preprints.org) | NOT PEER-REVIEWED | Posted: 17 October 2023 doi:10.20944/preprints202310.1005.v1

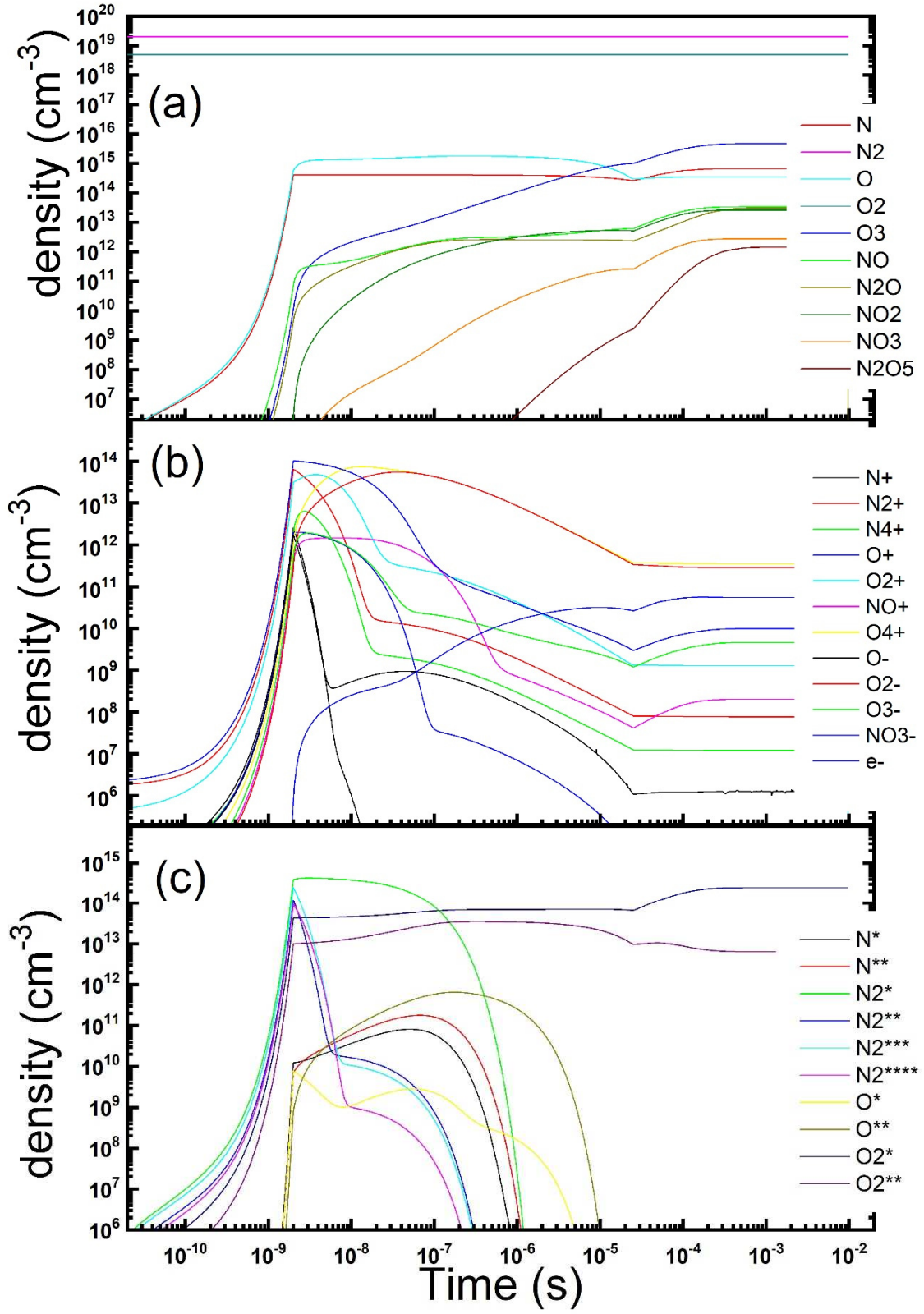

Figure 2. Temporal evolution of the gas phase composition under a repetitions of microdischarges in dry air: neutrals (**a**), charged (**b**) and metastables (**c**) species concentration is reported (parameters: T_e = 4 eV, $n_e = 1.2 \times 10^{14}$ cm^{-3}, τ_s = 2 ns, R_{str} = 100 μm, D_{gap} = 0.8 mm, τ_{rep} = 25 μs).

 doi:10.20944/preprints202310.1005.v1

3.1. Efficient ozone production

Ozone can be employed and actually is used in many processes, so there is scope to find better ways to produce it. Oxidation by ozone is quite efficient. In fact it was employed in water treatment as a powerful cleaning agent [29,30]. Many more applications of ozone have been proposed or introduced in medical treatments and in food sector applications. It was observed that already brief treatment times and small amounts of ozone are able to control infective agents, be it bacteria, molds, yeasts, viruses or other parasites. The ozone treatments were considered as a tool for contaminant inactivation on products such meat, eggs, fish, fruits, vegetables and dry foods [31,32]. Ozone has been proposed also in health treatments for instance in skin or other biological tissue, as an antimicrobial agent [33]. Other medical applications include dentistry for example [34].

When considering a model for pulsed operation mode, we need to make some definite choices decribing the kind of device setup that will be object of the simulation. In order to maintain the overall geometry implemented in the previously developed software we decide to define a cylindrical gas gap (like that one between two symmetric, equally insulated electrodes, consisting in a couple of parallel plates). The idealized device has an active volume made of a cylinder with diameter 35 mm and height 0.8 mm. According to an idealized parallel plane geometry, the electric field is considered as constant in intensity and directed parallel to the cylinder axis in the whole dicharge volume. Microdischarges in the form of thin channels aligned to the axis, like those discussed in the previous section, are thought to repeat with the same probability. This applies to each position in the considered discharge volume, ignoring any edge effect. The model will consider an effective repetition rate, which is connected by the period between subsequent active phases of the applied voltage. The effective rate value however is set by the ratio between the microdischarge affected volume and that of the whole device and also by the number of microdischarges that happens during each active phase. This could be rationalized as a model where all the microdischarges are equal to an average, typical one, which is uniquely defined by its assumed plasma parameters (the same employed in the model discussed insofar). Such a physical agent acts with a fixed, constant repetition rate and the same evolution is thought to happen at each position in the discharge volume (a so called zero-dimensional model of the plasma) [13]. It could appear as a roughly idealized simplification of the realistic device operations, but we feel that it does not overlook the relevant evolution and it makes more easy to check what is the overall inprint of plasma parameters, as they act on the discharge and device performances. As a matter of fact, a sort of uniformization of the gas gap composition is present also in the experiments because of diffusion processes. Also the great number of microdischarges and voltage cycles involved at different locations in the device volume produces a smearing of the overall performances. This is true even if experiments confirm that each microdischarge has a non-negligible variability in terms of amplitude, duration and delay between subsequent events [22]. As implied by the previous sentences, we have included diffusion processes outside the device volume, consisting in a mainly radial transport. They were added to the model in a straightforward way just as the diffusion outside the single streamer channel [25]. These simulations leads to results broadly in agreement with the evolution shown in Figure 2. So, the whole gap region reaches a steady composition with an equilibrium between outwards diffusion and production of ozone and other compounds due to the repeated discharge processes.

We are now in the position to introduce some ideal pulse operation. Again a few simplifications were implemented. The operating mode was imagined as consisting in a fixed number of equal active periods separated by quiet intervals. Based on the duration of the on (τ_{on}) and off (τ_{off}) periods, we can define a duty cycle, which was used as a figure of merit of the process. It is not surprising that the densities of the neutral species in the gas-phase show an evolution that broadly reproduces that already observed in continuous operation simulations. The important novelty is that, during the periods without discharges, ozone and nitrogen oxides accumulates while oxygen and nitrogen atoms are consumed as in the case of a single discharge afterglow. We were happy to constate that equilibrium is reached again in a few repetitions of duty cycles, generally less than some tens. This allows to maintain simulations length and machine times relatively affordably. The concentration reached by ozone at the end of the last pause period was estimated and displayed in Figure 3 as a

Preprints (www.preprints.org) | NOT PEER-REVIEWED | Posted: 17 October 2023 doi:10.20944/preprints202310.1005.v1

function of the pause period duration. It could be grasped how the ozone concentration increases, respect to the continuous repetition mode, with an optimal pause duration, before it decreases for too much longer pauses. When considered as a function of the power absorbed by the DBD reactor the effect is even more impressive, with a huge gain in the production efficiency and energy saving. Another quite interesting result lies in that the ozone concentraton reached is almost independent from the duration of the on period, in our case it was tested between 250 and 2000 μs. This arises from the steady state reached after a small number of repetitions. Any prolungation of the active time is just not needed.

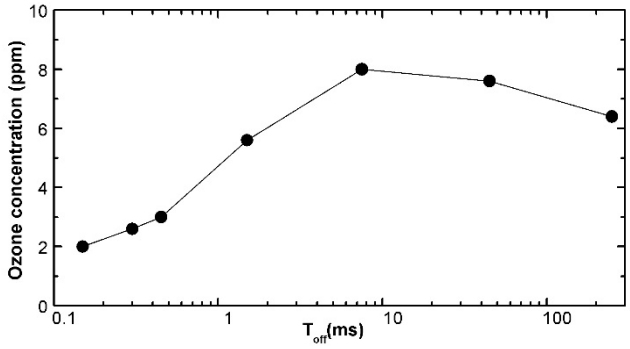

Figure 3. Ozone concentration in the gas phase as a function of the duration of the plasma-off phases between active plasma phases 450 μs long, each consisting of 18 repeated discharges with τ_{rep} = 25 μs (parameters: T_e = 4 eV, $n_e = 10^{12}$ cm^{-3}).

3.2. NOx remediation

The removal of NO and other nitrogen oxides from environment is a relevant problem concerning pollution control [35]. Nitrogen oxides stay in the low atmosphere for several days and enters cycles producing ozone, causing smog. Nitrogen oxides are mainly produced as by-product in combustion processes in free air. For instance in diesel engine exhaust NO can reach 200-500 ppm and NO_2 50 ppm [36]. On the other hand, understanding the capability of plasma treatment in the dissociation of such molecules, can provide some insight in the much more complex pattern involved in the plasma interaction with more harmful volatile compounds. So we slightly modified our simulations to consider the effect of plasma on a gas-phase composed of air contaminated by small levels of nitrogen oxides. In order to speed up the calculations, we neglected the contribution to dissociation given by excited states, for which the precise reaction rates with nitrogen oxides is also poorly known. No diffusion of contaminants from outside is considered here, to let the system reach the chemical equilibrium. Such a process kicks in however only at late times, both considering discharge repetition times (here 20 kHz, but several kHz generally). In Figures 4 we display the results of a simulation, with a continuous compared with a pulsed discharge. As we found previuosly [28] NO could be removed and transformed into ozone and to a smaller extent to other more oxidated states. In the reported simulations, we used the same plasma parameters as above, but we started form a gas-phase containing 500 ppm of NO, that is a density of 1.3×10^{16} cm^{-3}. After a few discharges, NO starts to decline and gets almost completely removed in a short period, oxidated initially by O atoms and then, when atomic radicals disappear, con sumed in reactions with ozone and NO_2. In the final state it is substituted mainly by ozone (about 10 ppm). A small amount of NO_2 (1.6 ppm) and N_2O (0.8 ppm) is produced too, while other oxides do not form with appreciable concentration. NO equilibrium level is down to 0.8 ppm. From the figure, it could also be appreciated that transition in th gas-phase takes more times, respect to those involved in ozone formation. From the time evolution point of view, we observe that, while the transition from oxygen atoms to ozone happens after about 10 μs, NO transition to ozone starts only after 175 μs and equilibrium is reached after about 0.5 ms. The overall effect of the duty-cycleis not immediately perceivable. However a closer look reveals its effects. Part of the NO equilibrium concentration is build up by the plasma itself. In this case the

Preprints (www.preprints.org) | NOT PEER-REVIEWED | Posted: 17 October 2023 doi:10.20944/preprints202310.1005.v1

application of a 50% duty cycle (see Figure 4) could improve the reduction of the NO level (here 0.1 and 0.5 ppm after the off/on phases) besides cutting to half the energy consumed.

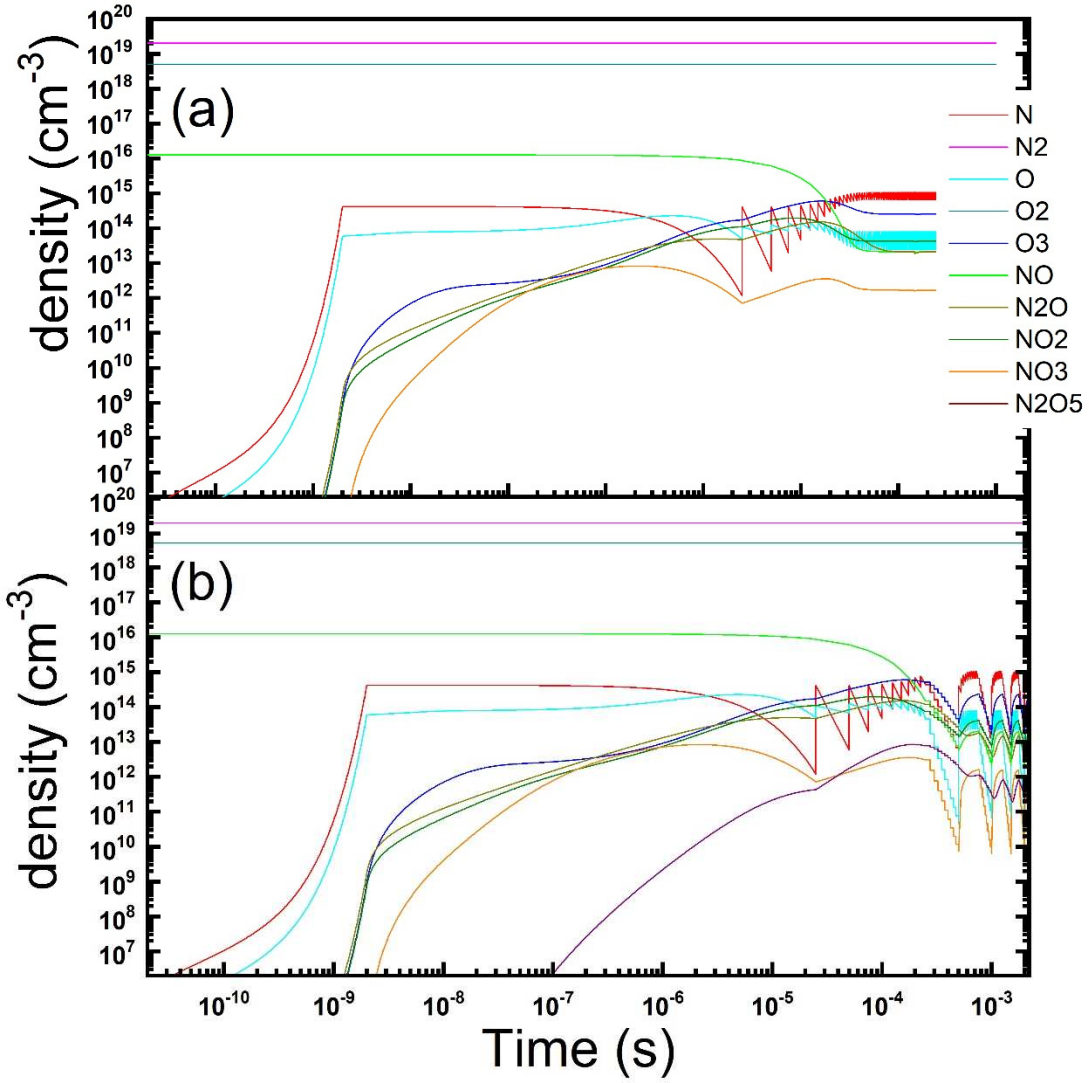

Figure 4. Temporal evolution of the gas phase composition under a repetitions of microdischarges in dry air contaminated by NO: continuous (**a**) vs pulsed (**b**) discharge operation is reported (parameters: T_e = 4 eV, n_e = 1.2 × 10^{14} cm^{-3}, τ_s = 2 ns, R_{str} = 100 μm, D_{gap} = 0.8 mm, τ_{rep} = 25 μs, duty-cycle: 10 on/10 off discharges).

3.3. Water vapour dissociation

A step forward could be done, by extending the modeling to perform simulations of humid air plasma gas-phase. That required a substantial expansion of both the number of species considered and of their reaction database [14,37]. Based again on available experimental informations, we gathered a set including 20 neutral and 21 charged states, with 667 reactions. In a preliminary effort, again excited molecules were excluded. Here we presents only a few results to demonstrate the potential of the model. The density of the neutral and charged species is displayed in a log-log scale as a function of time in Figure 5, using the same parameters already shown for the dry air simulations, but now with a water vapour partial pressure of 1 mbar. A pattern similar to dry air conditions could be recognized also in the wet atmosphere. After a few microseconds, the main product remains ozone, whereas the charge phase consists primarily of oxygen positive and negative ions. However, here the 0.1% concentration of water vapour is sufficient to affect deeply the details. NO^+ and H_3O^+ ions becomes significant and slowly adds to the ions phase, while, albeit only partially, OH^- negative ions grows. Hydrogen ions remain minority

Preprints (www.preprints.org) | NOT PEER-REVIEWED | Posted: 17 October 2023 doi:10.20944/preprints202310.1005.v1

and a small amount of ammonia NH_4^+ is formed also. We could inspect now, the behavior of the neutral gas-phase, displayed in Figure 5a. The main chemical kinetics effect remains the reaction of atomic oxygen to produce mainly ozone, with some concentration of nitrogen oxides. In wet air, however, even starting with such a limited amount of water vapour is sufficient to alter the evolution. Ozone formation is somewhat inhibited, reaching only 10 ppm concentration. Production of hydrogen or ammonia appears to be disfavoured, with only a trace of HNO molecules, slowly building up. Atomic oxygen, but also atomic hydrogen and oxydril radicals react and get consumed. The other main components of the gas-phase turn out to become nitrogen oxides (N_2O, NO and NO_2 mainly, compared to NO_3 and N_2O_5) and hydrogenated water (O_2H favoured more than H_2O_2 itself), whose limited reactivity allows accumulation. At higher initial water vapour concentrations, ozone is substituted by those compounds in the final neutral gas-phase. This pattern of chemical kinetics appears to be substantially solid. It could be traced by increasing water vapour concentration or the neutral gas temperature, which allows to investigate even larger wet conditions as vapour pressure is increased. The transition from dry to wet air plasma conditions, characterized by the substitution of ozone and nitrogen oxide ions in favour of species originated from water, can be set at around 1% water vapor concentration. How this pattern is modified by applying a pulsed regime of discharges, could be observed from the trends displayed in Figure 6.

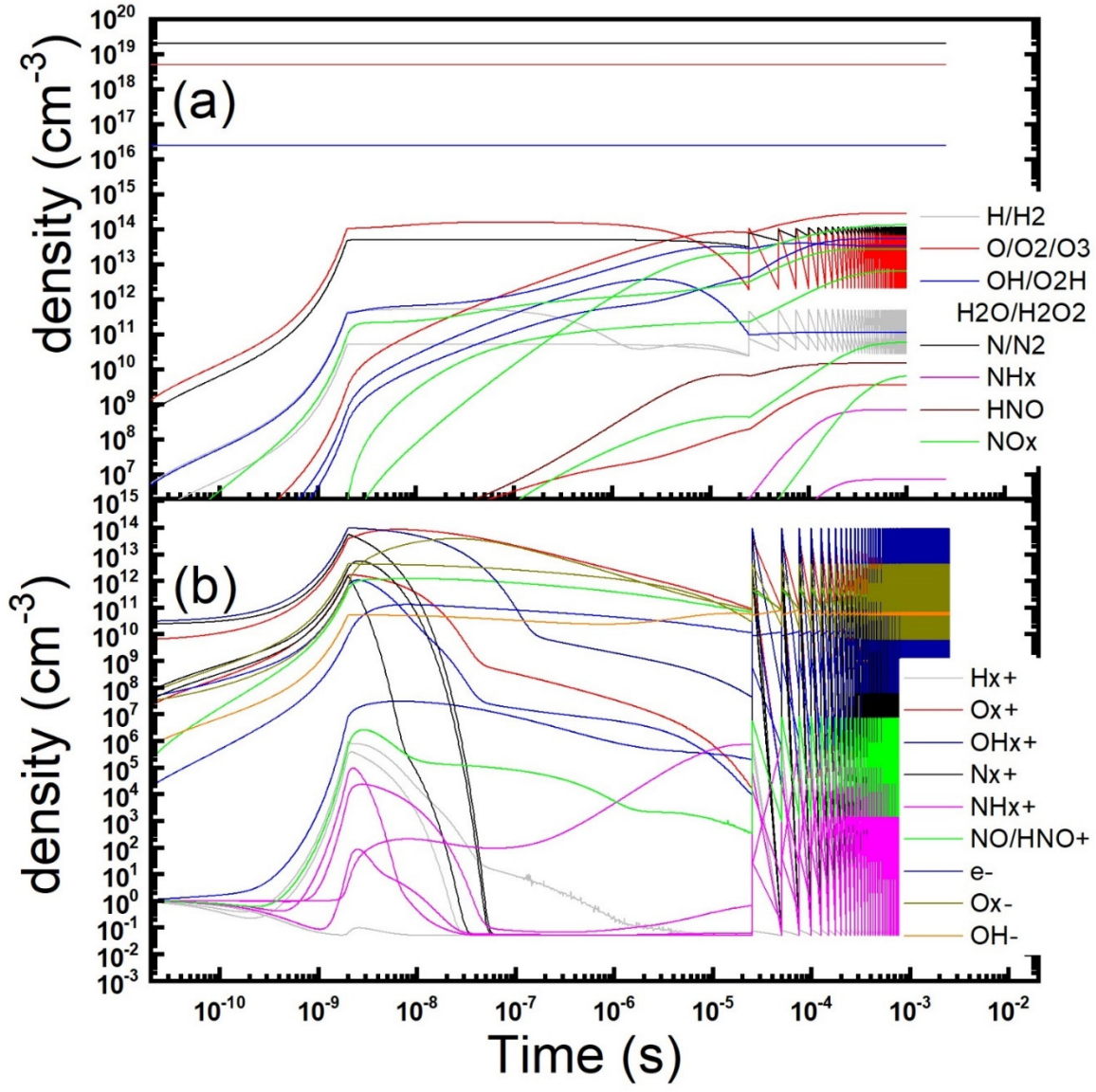

Figure 5. Temporal evolution of the gas phase composition under a repetitions of microdischarges in wet air: neutrals (**a**) and charged (**b**) species concentration is reported (parameters: T_e = 4 eV, n_e = 1.2 × 10^{14} cm^{-3}, τ_s = 2 ns, R_{str} = 100 μm, D_{gap} = 0.8 mm, τ_{rep} = 25 μs).

Preprints (www.preprints.org) | NOT PEER-REVIEWED | Posted: 17 October 2023 doi:10.20944/preprints202310.1005.v1

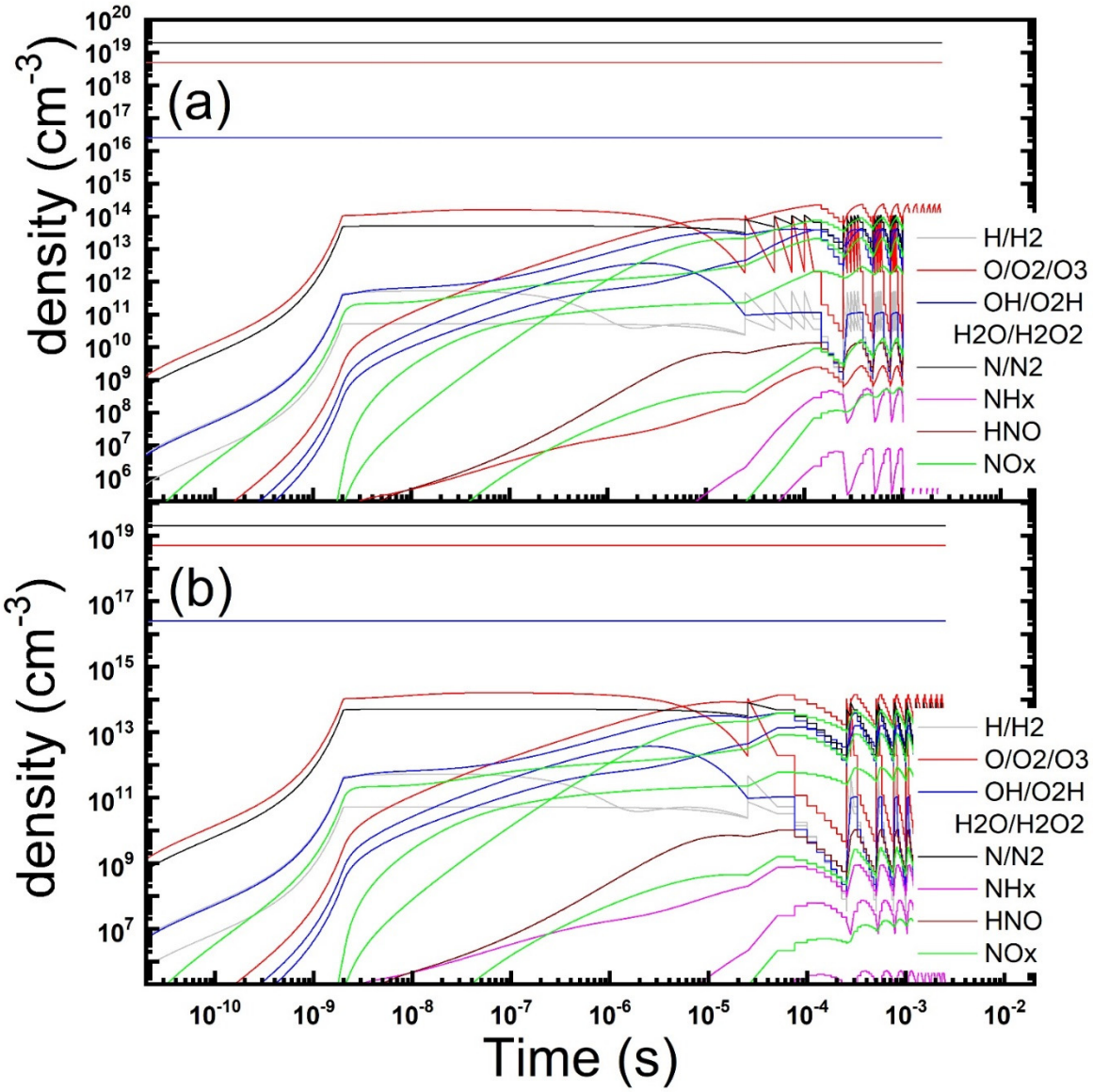

Figure 6. Temporal evolution of the gas phase composition under a repetitions of microdischarges in wet air with pulsed discharge operation is reported (parameters: T_e = 4 eV, n_e = 1.2 × 10^{14} cm^{-3}, τ_s = 2 ns, R_{str} = 100 μm, D_{gap} = 0.8 mm, τ_{rep} = 25 μs, duty-cycle: 5 on/5 off (**a**) and 2 on/8 off (**b**) discharges).

A duty cycle of 5:5 and 2:8 on:off discharges was applied. As it could be guessed, the final gas-phase looks similar, but we observe once more an increase in the final output of ozone using a lower amount of energy for the electrical discharges. The efficiency is higher by 65% and 150% in the two instances.

3.4. Ammonia treatment

As a by-product of the wet air chemical kinetics environment, our simulations allow to discuss another interesting point. As stated before, a meaningful description of the plasma gas phase include hydrogen and ammonia compounds too. So the model could be used also to discuss the chemical kinetics of discharges containing ammonia in the initial mixture. This chemical could be harmful at high concentrations and it is produced in a variety of precess both natural and industrial [38]. This could also provide some insight in the much more complex pattern involved in the plasma interaction with more harmful volatile compounds.

The results of the simulation is displayed in Figure 7, where the density of the neutral species is reported in a log-log scale as a function of time. In the bottom frame a duty cycle of 2:8 on:off discharges was applied and compared with a continuous discharge. The modeling was evaluated

Preprints (www.preprints.org) | NOT PEER-REVIEWED | Posted: 17 October 2023 doi:10.20944/preprints202310.1005.v1

with the same parameters already shown for the dry and wet air simulations, but now with an ammonia partial pressure of about 0.2 mbar, correponding to 22 ppm [14].

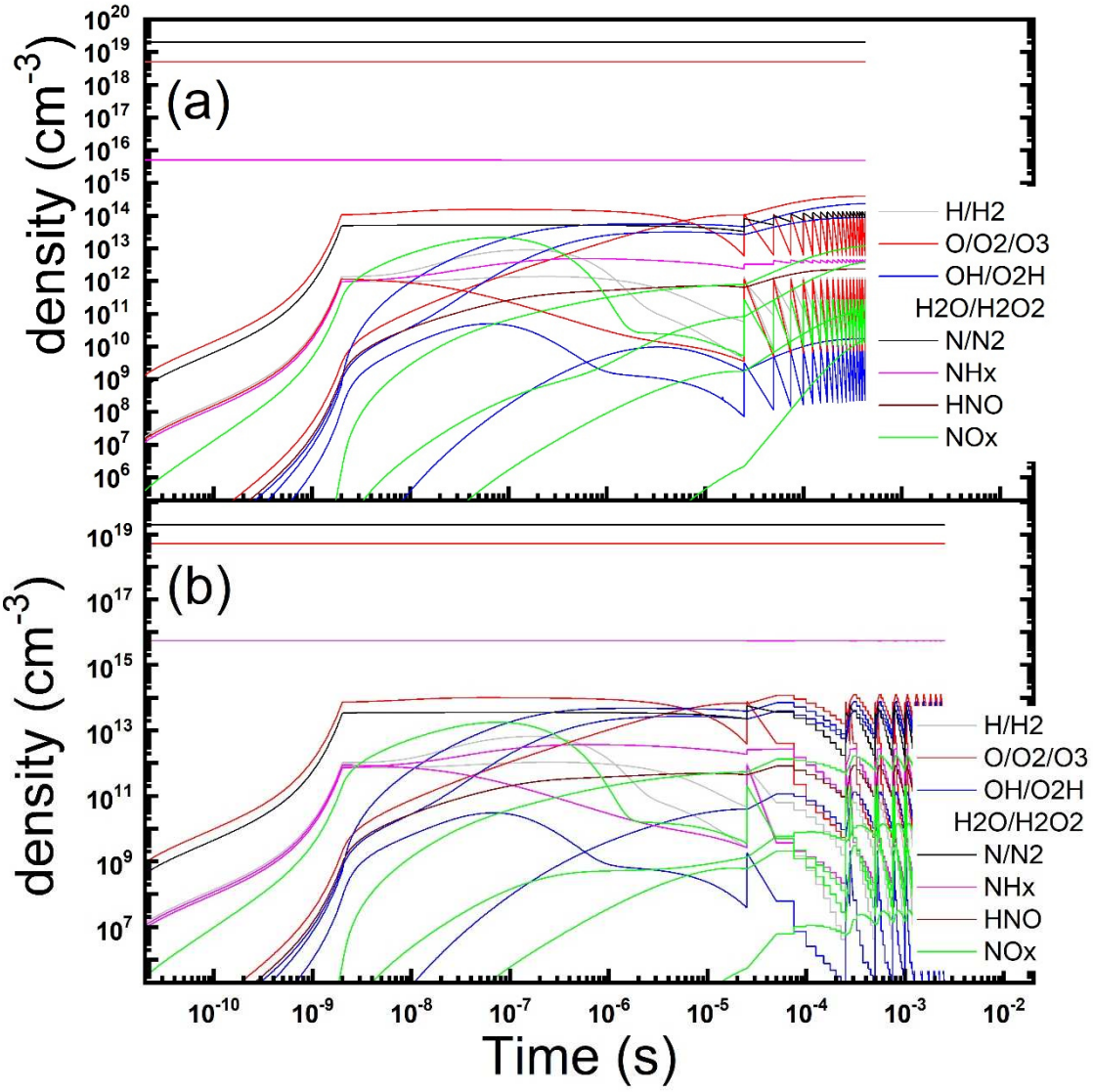

Figure 7. Temporal evolution of the gas phase composition under a repetitions of microdischarges in dry air contaminated by ammonia: continuous (**a**) vs pulsed (**b**) discharge operation is reported (parameters: T_e = 4 eV, n_e = 1.2 × 10^{14} cm^{-3}, τ_s = 2 ns, R_{str} = 100 μm, D_{gap} = 0.8 mm, τ_{rep} = 25 μs, duty-cycle: 10 on/10 off discharges).

The equilibrium gas-phases look similar and ammonia is consumed to produce mainly ozone and water vapour and its radicals. On the other hand, ammonia radicals (majority NH_2) as well as nitrogen oxides (majority NO_2 and N_2O) reach only small concentrations. Even smaller is the more harmful nytroxyl radical HNO. So the plasma remediation process appears to be nicely clean and quite efficient too. As already observed, the application of the duty cycle substantailly lower the amount of energy necessary for the transformation of the same quantity of ammonia by the electrical discharge. The efficiency is higher by 67% by using the 2:8 duty cycle. The simulation provides also interesting features in the evolution of the neutral and charged gas-phase which help understanding the reaction pattern of ammonia, with a substantial room for treatment process improvement.

 doi:10.20944/preprints202310.1005.v1

3.5. Addressing air purification treatments

Finally we discuss the use of such kind of modeling in a more realistic environment, linked to existing plasma devices and processes. The aim was to draw a comparison with the findings of an experimental campaign, aimed to VOC remediation and air purification [11,39]. The device and its properties are discussed elsewhere [10], so we report briefly only the relevant features needed to implement a few targeted simulations. The discharges happens at the surface of a stacked set of teflon plates. Electrodes consists of five parallel, equally spaced, metal stripes, 75 mm long, glued and exposed on the upper surface, while an insulated metal plate on the lower surface acts as ground electrode. This configuration is typical of surface DBD, used previously to study ion wind and plasma aerodynamics [16]. An air flow (14 L/s) is maintained in a pipe (12 cm diameter) streaming along the electrodes, so that discharges happens mostly transverse to the flow direction. Discharge repetition rate was 4 kHz.

As for the simulations, the model could be formulated as a plug-flow reactor [22]. Considering the experimental flow-rate, the global exposure time to the plasma is then 60 ms. The streamer channel was considered as rectangular, with 100 μm square section, to simplify the treatment of diffusion, and covering the inter-electrode space. Diffusion and reactions onto the dielectric surfaces are to be considered here. However, since the discharge repetition frequency is substantially larger than the crossing time of the microdischarge channel, the system could be modeled as a repetition of independent discharge events, just as we have discussed insofar. The peak electron density was estimated from experimental data on the charge transported by the microdischarges [10].

The results of the simulation is displayed in Figure 8, where the density of the neutral and charged species is reported in a log-log scale as a function of time. It could be observed that the relevant trends in the evolution of the gas-phase are similar to those obtained in the symmetric DBD setup discussed previously. So, this kind of simulations can be used as a guide also in more complex and realistic experimental geometries and setups. More detailed comparisons between experiments and simulations will be addressed in a future dedicated work.

Preprints (www.preprints.org) | NOT PEER-REVIEWED | Posted: 17 October 2023 doi:10.20944/preprints202310.1005.v1

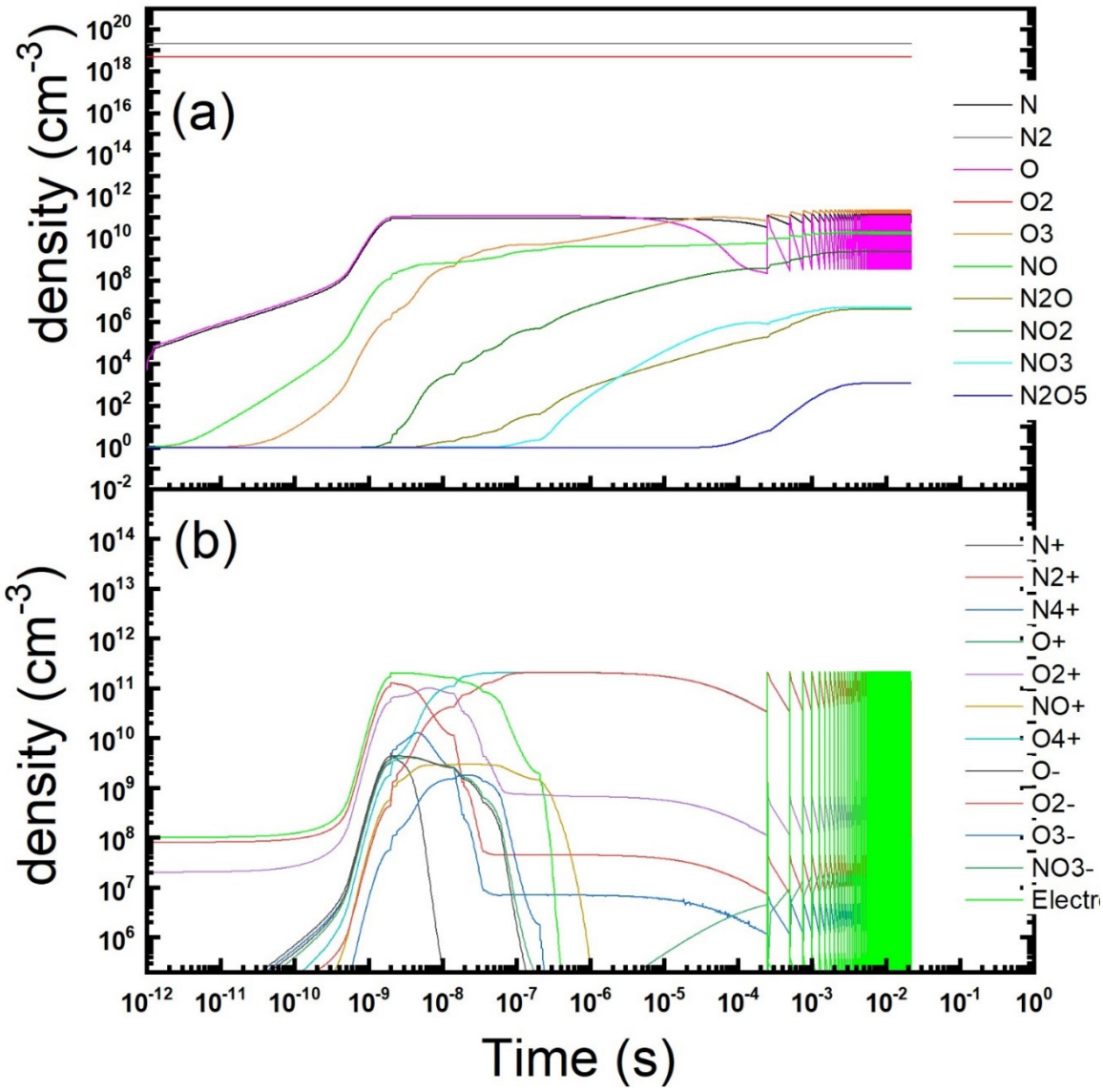

Figure 8. Temporal evolution of the gas phase composition under a repetitions of microdischarges in dry air under the conditions of experiments reported in Ref. [10]. Simulation plasma parameters: T_e = 4 eV, $n_e = 2 \times 10^{11}$ cm^{-3}. τ_s = 2 ns.

4. Discussion and Conclusions

We have presented several issues that could be analysed in the framework of chemical kinetics simulations of dielectric barrier discharge plasmas. In particular we have focused on the role of pulsed operation in the control of the evolution of the discharge gas-phase. We have demonstrated that interesting effects could be achieved, when the pulse times are comparable with the relevant scales for the formation of stable molecular species. We discussed instances relative to ozone, nitrogen oxides, water vapour and ammonia.

Taking a more general point of view, simplified but reasonably fast simulations of the plasma chemical kinetics can bring fruitful informations about the pattern taken by the gas-phase evolution, which could the experimental campaign and help to design the device (electrode spacing and number, relative to the flowrate to be processed) and the operating conditions. As we have in this work, carefully designed duty cycles help to substantially reduce the electrical power consumption and to boost the process efficiency, possibly achieving an economic viability of plasma processing, this being the main brake to the spreading of this kind of technology [1].

Author Contributions: Conceptualization, C.R.; methodology, R.B.; software, R.B. and A.P.; validation, R.B. and A.P.; resources, C.R.; writing—original draft preparation, R.B.; writing—review and editing, R.B. and C.R.; visualization, R.B.; supervision, C.R.; project administration, C.R.; funding acquisition, C.R. All authors have read and agreed to the published version of the manuscript.

Funding: Part of the research was performed within the MUSA—Multilayered Urban Sustainability Action—project, funded by the European Union—NextGenerationEU, under the National Recovery and Resilience Plan (NRRP) Mission 4, Component 2, Investment Line 1.5: Strenghtening of research structures and creation of R&D "innovation ecosystems", set up of "territorial leaders in R&D". A.P. would also acknowledge the support received by Milano-Bicocca University in the project Bicocca Starting Grant - 2020, where he was P.I.

Data Availability Statement: The data presented in this study are available on request from the corresponding author.

Acknowledgments: We are pleased to acknowledge the support of our technical staff at the PlasmaPrometeo Center, Alessandro Mietner and Alessandro Bau.

Conflicts of Interest: The funders had no role in the design of the study; in the collection, analyses, or interpretation of data; in the writing of the manuscript, or in the decision to publish the results.

References

1. Kogelschatz, U. Dielectric-barrier discharges: Their history, discharge physics, and industrial applications. *Plasma Chem. Plasma Proc.* **2003**, *23*, 1-46.
2. Brandenburg, R. Dielectric barrier discharges: Progress on plasma sources and on the understanding of regimes and single filaments. *Plasma Sources Sci. Technol.* **2017**, *26*, 053001.
3. Fridman, A.; Chirokov, A.; Gutsol, A. Non-thermal atmospheric pressure discharges. *J. Phys. Appl. Phys.* **2005,** *38,* R1.
4. Li, J.; Ma, C.; Zhu, S.; Yu, F.; Dai, B.; Yang, D. A Review of Recent Advances of Dielectric Barrier Discharge Plasma in Catalysis. *Nanomaterials* **2019**, *9*, 1428.
5. Napartovich, A.P. Overview of Atmospheric Pressure Discharges Producing Nonthermal Plasmas. *Plasmas and Polymers*, 2001, *6*, 1-14.
6. Starikovskaia, S.M.; Anikin, N.B.; Pancheshnyi, S.V.; Zatsepin, D.V.; Starikovskii, A.Y. Pulsed Breakdown at High Overvoltage: Development, Propagation and Energy Branching. *Plasma Sources Sci. Technol.* **2001**, *10*, 344.
7. Wang, Q.; Liu, F.; Miao, C.; Yan, B.; Fang, Z. Investigation on discharge characteristics of a coaxial dielectric barrier discharge reactor driven by AC and ns power sources. *Plasma Science and Technology*, **2018**, *20*, 035404.
8. Barni, R.; Esena, P.; Riccardi, C. Chemical kinetics simulation for atmospheric pressure air plasmas in a streamer regime. *Journal of Applied Physics,* **2005,** *97*, 073301.
9. Riccardi, C.; Barni, R. Chemical kinetics in air plasmas at atmospheric pressure. In *Chemical Kinetics*, Patel, V., Eds.; Intech: Rijeka, **2012**, pp. 185-202.
10. Piferi, C.; Barni, R.; Roman, H.E.; Riccardi, C. Current Filaments in Asymmetric Surface Dielectric Barrier Discharge. *Applied Science,* **2021**, *2021*, 2079.1-22.
11. Piferi, C.; Brescia, A.; Riccardi, C. Intensity comparison between UV lamps and plasma emission for air purification studies. *AIP Advances* **2021**, *11*, 085209.
12. Kulikovsky, A.A. Positive streamer in a weak field in air: A moving avalanche-to-streamer transition. *Phys. Rev. E* **1998**, 57, 7066.
13. Tanaka, Y. Prediction of dielectric properties of N2/O2 mixtures in the temperature range of 300–3500K. *J. Phys. D: Appl. Phys*., **2004**, *37*, 851–859.
14. Barni, R.; Dell'Orto, E.; Riccardi, C. Chemical kinetics of the plasma gas-phase in humid air non-thermal atmospheric pressure discharges. *Int. J. Plasma Environmental Science and Technology,* **2019**, *12,* 109-113.
15. Soloshenko, I.A.; Tsiolko, V.V.; Pogulay, S.S.; Kalyuzhnaya, A.G.; Bazhenov, V.Y.; Shchedrin, A.I. Effect of water adding on kinetics of barrier discharge in air. *Plasma Sources Sci. Technol.* **2009**, 18, 045019.
16. Biganzoli, I.; Barni, R.; Riccardi, C.; Gurioli, A.; Pertile, R. Optical and Electrical Characterization of a Surface Dielectric Barrier Discharge Plasma Actuator. *Plasma Sources Sci and Technol.*, **2013**, *22*, 025009.1-9.
17. Biganzoli, I.; Barni, R.; Riccardi, C. Temporal evolution of a surface dielectric barrier discharge for different groups of plasma microdischarges. *J. Phys. D: Appl. Phys***. 2013**, 46, 025201.
18. Ito, T.; Kanazawa, T.; Hamaguchi, S. Rapid Breakdown Mechanisms of Open Air Nanosecond Dielectric Barrier Discharges. *Physical Review Letters*, **2011**, *107*, 065002.1-4.
19. Biganzoli, I.; Barni, R.; Riccardi, C.; Gurioli, A.; Pertile, R. Experimental investigation of Lissajous figure shapes in planar and surface dielectric barrier discharges. *J. Phys. - Conf. Series* **2014,** *550*, 012039.1-10.
20. Starikovskaia, S.M.; Allegraud, K.; Guaitella, O.; Rousseau, A. On electric field measurements in surface dielectric barrier discharge. *Journal of Physics D,* **2010,** *43*, 124007.1-5.

21. Raizer, Y.P. *Gas Discharge Physics;* Springer: Heidelberg, Germany, 1991.
22. Barni, R.; Biganzoli, I.; Dell'Orto, E.; Riccardi, C. Effect of Duty-Cycles on the Air Plasmas Gas-Phase of Dielectric Barrier Discharges. *Journal of Applied Physics,* **2015,** *118*, 143301.1-13.
23. Biganzoli, I.; Barni, R.; Riccardi, C. On the use of Rogowski coils as current probes for atmospheric pressure dielectric barrier discharges. *Review of Scientific Instruments,* **2013,** *84*, 016101.1-3.
24. Benson, S.W. *Thermochemical Kinetics*; Wiley: New York, US, **1982**.
25. Chantry, P. J. A simple formula for diffusion calculations involving wan reflection and low density, *J. Appl. Phys.*, **1987**, *62*, 1141.
26. Marinov, D.; Guerra, V.; Guaitella, O.; Booth, J-P.; Rousseau, A. TITLE. *Plasma Sources Sci. Technol.*, **2013**, *22*, 055018.
27. Popov, N.A. Vibrational kinetics of electronically-excited N2(A,v) molecules in nitrogen discharge plasma. *J. Physics D* **2013**, *46*, 355204.
28. Barni, R.; Riccardi, C. Perspective of NOx removal from numerical simulation of non-thermal atmospheric pressure plasma chemical kinetics. *High Temperature Material Processes,* **2010**, *14,* 205-210.
29. Pavlovich, M.J.; Chang, H.W.; Yukinori, S.; Clark, D.S.; Graves, D.B. Ozone correlates with antibacterial effects from indirect air dielectric barrier discharge treatment of water. *J. Phys. D: Appl. Phys*. **2013,** 46, 145202.1-12.
30. Barni, R.; Biganzoli, I.; Dell'Orto, E.; Riccardi, C. Effects of a pulsed operation on ozone production in dielectric barrier air discharges. *Letters in Applied NanoBioScience* **2014**, *3*, 167-171.
31. Application Food, something more modern 1999-2004.
32. Hayes, J.; Kirf, D.; Garvey, M.; Rowan, N. Disinfection and toxicological assessments of pulsed UV and pulsed-plasma gas-discharge treated-water containing the waterborne protozoan enteroparasite Cryptosporidium parvum. *J. Microbiological Methods* **2013**, 94, 325-337.
33. Azarpazhooh, A.; Limeback, H. The application of ozone in dentistry: A systematic review of literature, *J. Dentistry* **2008**, 36, 104-116.
34. Valacchi, G.; Fortino, V.; Bocci, V. The dual action of ozone on the skin. *British Journal of Dermatology* ***2005***, 153, 1096-1100.
35. Amoroso, A.; Beine, H.J.; Esposito, G.; Perrino, C.; Catrambone, M.; Allegrini, I. Seasonal differences in atmospheric nitrous acid near Mediterranean urban areas. *Water Air and Soil Pollution* **2008**, 188, 81.
36. Srinivasan, A.D.; Rajanikanth, B.S. Nonthermal-Plasma-Promoted Catalysis for the Removal of From a Stationary Diesel-Engine Exhaust. *IEEE Trans. Ind. Appl.* 2007, 43, 1507.
37. Barni, R.; Roman, H.E.; Citterio, A.; Leonardi, G.; Riccardi, C. Atmospheric Plasma Treatments of Cashmere: The Role of Nanoscale Sizing in the Spray Coating Processing. *Frontiers in Materials* **2022,** 9, 987608.1-15.
38. Mehta, P.; Barboun, P.; Herrera, F.A.; Kim, J.; Rumbach, P.; Go, D.B.; Hicks, J.C.; Schneider, W.F. Overcoming ammonia synthesis scaling relations with plasma-enabled catalysis. *Nature Catalysis* **2018**. 1, 269–275.
39. Zanini, S.; Zoia, L.; Della Pergola, R.; Riccardi, C. Pulsed plasma-polymerized 2-isopropenyl-2-oxazoline coatings: Chemical characterization and reactivity studies. *Surface and Coatings Technology* **2018,** 334, 173.